Dihydrotanshinone exerts antitumor effects and improves the effects of cisplatin in anaplastic thyroid cancer cells

LORENZO ALLEGRI[1], ROSSANA DOMENIS[1], MICHELE NAVARRA[2], MARILENA CELANO[3], DIEGO RUSSO[3], FRANCESCA CAPRIGLIONE[3], GIUSEPPE DAMANTE[1,4] and FEDERICA BALDAN[1]

[1]Department of Medicine, University of Udine, I-33100 Udine; [2]Department of Chemical, Biological, Pharmaceutical and Environmental Sciences, University of Messina, I-98122 Messina; [3]Department of Health Sciences, University of Catanzaro 'Magna Graecia', I-88100 Catanzaro; [4]Institute of Medical Genetics, 'Academic Hospital of Udine', I-33100 Udine, Italy

Received May 19, 2020; Accepted June 3, 2021

DOI: 10.3892/or.2021.8155

Abstract. Anaplastic thyroid cancer (ATC) is the most aggressive type of thyroid cancer and is responsible for 20-50% of thyroid cancer-associated deaths. The absence of response to conventional treatments makes the search for novel therapeutics a clinical challenge. In the present study, the effects of 15,16-dihydrotanshinone I (DHT), a tanshinone extracted from *Salvia miltiorrhiza* Bunge (Danshen), which has previously been shown to possess anticancer activity, were examined in two human ATC cell lines. DHT significantly reduced cell viability, which was coupled with an increase in apoptosis. DHT administration also reduced the colony-forming ability and proliferation of these cells in soft agar and downregulated the expression of epithelial-to-mesenchymal transition-related genes. In addition, DHT significantly reduced *MAD2* expression, a target of HuR with a relevant role in ATC. Finally, cotreatment with cisplatin and DHT has a greater effect on cell viability than each compound alone. In conclusion, to the best of our knowledge, the present study is the first to demonstrate that DHT exerts antitumor effects on ATC cells by reducing *MAD2* expression levels. Moreover, a synergistic effect of DHT with cisplatin was shown. Further *in vivo* studies are required to assess this phytochemical compound as a potential adjuvant for the treatment of ATC.

Introduction

Thyroid cancer accounts for 1-2% of all cancer cases worldwide, representing the most prevalent type of endocrine malignancy (1,2). Most thyroid carcinomas are derived from follicular cells and are classified into three broad categories based on their differentiation levels: i) Differentiated thyroid cancer (DTC), including papillary thyroid cancer (PTC) and follicular thyroid cancer (FTC); ii) poorly DTC and undifferentiated thyroid cancer; and iii) anaplastic thyroid cancer (ATC) (1). ATC is a rare, but aggressive, form of thyroid malignancy. Indeed, despite the fact that it only accounts for <2% of all thyroid malignancies, it is responsible for 20-50% of thyroid cancer-associated deaths (thyroid cancer incidence and mortality in the United States, 1974-2013) (1,2). Due to the fast-growing and aggressive nature of the tumor, the majority of patients with ATC are diagnosed with stage-IV disease, at which point surgery is not possible (3). Moreover, due to its undifferentiated nature, ATC is not sensitive to the conventional treatments used for well-differentiated thyroid cancers, such as radioactive iodine ablation, as thyroid-specific gene expression is lost through the dedifferentiation process (4,5). Thus, the median survival rates in several population-based studies have been reported to be between 3 and 6 months, without evidence of any improvement over several decades (6,7). Treatments with widely used chemotherapeutic agents, such as doxorubicin or cisplatin, as well as more recent taxane-based therapies, are unable to improve the poor overall survival rates, primarily due to inadequate control of distant metastases (8,9). Novel strategies are currently under investigation, including a major effort to identify innovative approaches to ATC management.

Phytochemicals, a large class of chemical substances naturally produced in plants, have been demonstrated to exhibit several biological properties, including anticancer effects (10,11). In this context, in the field of thyroid cancer, resveratrol has been shown to sensitize tumor cells to radioiodine therapy (12). Furthermore, in the case of curcumin, the capacity to inhibit invasion and migration via downregulation of the PI3K/Akt signaling pathway has been reported in FTC cells (13) and inhibition of TGF-β1-induced epithelial-to-mesenchymal transition (EMT) has been reported in PTC cells (14). In consideration of these findings, testing novel plant extracted compounds in thyroid cancer therapy appears to be a promising strategy. Recently, among the more novel extracted plant compounds with anticancer activity, particular attention has been placed on 15,16-dihydrotanshinone I (DHT), a tanshinone extracted from *Salvia miltiorrhiza* Bunge (Danshen), one

Correspondence to: Professor Giuseppe Damante, Department of Medicine, University of Udine, Building E Via Chiusaforte, I-33100 Udine, Italy
E-mail: giuseppe.damante@uniud.it

Key words: thyroid cancer, HuR, phytochemical, MAD2, cisplatin

of the most frequently prescribed herbs in Traditional Chinese Medicine (15). DHT possesses anticancer activity in different types of cancer, including colon (16), breast (17) and gastric cancer (18), with an effective dose 50 (ED_{50}) <10 μM (15-18). DHT has been reported to be able to induce cell cycle arrest at the S and G_1 phases (17), as well as apoptosis, acting primarily through the BCL2 family of proteins (19). In addition, DHT has also been tested in animal models, confirming its ability to inhibit tumor growth in xenograft nude mouse models, without adverse effects on other tissues (20,21). Notably, DHT is effective in reducing cell proliferation and aggressiveness, even in some drug-resistant tumor cell lines, such as K562/ADR cells, and in p-glycoprotein-overexpressing HepG2 subclones (22). DHT has been reported to enhance the effectiveness of irradiation, as the combination of irradiation and DHT induces significantly greater decrease in tumor growth in a nude xenograft mouse model of cervical cancer (23).

Previously, Lal *et al* (24) showed that DHT treatment modifies the activity of HuR, an RNA-binding protein involved in tumorigenesis and cancer progression, altering its binding to mRNA targets *in vivo*. In our previous studies, HuR was overexpressed in thyroid cancer and that its downregulation resulted anticancer effects in ATC cell lines (25-27).

Altogether, these findings indicate that DHT may be a potential candidate for ATC treatment. Thus, in the present study, the effects of DHT were examined in two human ATC cell lines. As it has been established that DHT inhibits HuR-target interactions (24), the aim of the present study was to evaluate the effects of DHT on MAD2, a key component of the MAD/BUB complex that regulates sister-chromatid separation during metaphase to anaphase progression (28), and a known target of HuR with a relevant role in cancer progression (27). The effect of the combination of DHT with cisplatin were also investigated.

Materials and methods

Cell lines. SW1736 and 8505C cells, derived from ATC (29-31), were cultured in RPMI-1640 medium (Euroclone S.p.A) supplemented with 10% FBS (Gibco; Thermo Fisher Scientific, Inc.), 2 mM L-glutamine (Euroclone S.p.A) and 50 mg/ml gentamicin (Gibco; Thermo Fisher Scientific, Inc.). Cells were cultured in a humidified incubator (5% CO_2 and 95% air at 37˚C). Both cell lines were validated using short tandem repeat analysis and confirmed to be mycoplasma-free. SW1736 and 8505C cells were treated with DMSO (vehicle; Sigma-Aldrich; Merck KGaA), DHT (Selleck Chemicals) or cisplatin (Cayman Chemical Company).

Cell viability. In order to test cell viability, the MTT assay was used. SW1736 and 8505C cells ($4x10^3$ cells/well) were seeded in 96-well plates. The following day, cells were treated with DHT (0.5, 1, 2 or 3 μM) and cisplatin (1 μM) at different concentrations. After 24, 48 or 72 h of incubation, 4 mg/ml MTT (Sigma-Aldrich; Merck KGaA) was added to the cell medium and cells were cultured for a further 4 h in the incubator in the dark. The supernatant was removed, 100 μl/well DMSO (Sigma-Aldrich; Merck KGaA) was added, and the absorbance at 570 nm was measured. All experiments were performed as six technical repeats and cell viability is expressed as the fold-change relative to the control (DMSO-treated cells).

Cell cycle analysis. Cell cycle distribution was determined using flow cytometry analysis of DNA content, as previously described (32). Briefly, SW1736 and 8505C cells were treated with 1.5 μM DHT or DMSO for 48 h. The cells were collected and fixed in cold 70% ethanol, then stained with propidium iodide solution containing RNase and Triton-X100 at 4˚C for 30 min. Flow cytometry analysis was performed on a FACSCalibur instrument (BD Biosciences) using ModFit LT 5.0 analysis software (Verity Software House, Inc.). A minimum of $2x10^4$ cells were analyzed for each sample. All experiments were performed in triplicate.

Annexin V and propidium iodide assay. To assess the effects of DHT on cell death, an Annexin V and propidium iodide assay was performed using the eBioscience Annexin V-FITC Apoptosis Detection kit (cat. no. 88-8005-74; Thermo Fisher Scientific, Inc.), according to the manufacturer's protocol. Briefly, DHT-treated SW1736 and 8505C cells were washed with cold PBS and resuspended in 195 μl binding buffer (BB; 10 mM; HEPES/NaOH, pH 7.4; 140 mM NaCl and 2.5 mM $CaCl_2$). A total of 5 μl fluorescein isothiocyanate-conjugated Annexin V (Annexin V-FITC) was added and samples were incubated for 10 min at room temperature. After washing, cells were resuspended in 190 μl BB in which 10 μl propidium iodide stock solution (final concentration 1 μg/ml) were added. Flow cytometry analysis was performed on a FACSCalibur (Becton-Dickinson and Company) and analyzed using the Summit software (Beckman-Coulter). All experiments were performed in triplicate.

Protein extraction and western blotting. Total protein was extracted from SW1736 and 8505C cells, treated with 1.5 μM DHT or DMSO, using a cell scraper and lysis buffer (50 mM Tris HCl, pH 8; 120 mM NaCl; 5 mM EDTA; 1% Triton; 1% NP40; 1 mM DTT), supplemented with phenyl-methylsulphonyl fluoride and protease inhibitors. Lysates were centrifuged at 13,000 x g for 10 min at 4˚C, and supernatants were quantified using a Bradford assay.

For western blot analysis, 30 μg protein was loaded per lane on a 10% SDS gel, resolved using SDS-PAGE, then transferred to nitrocellulose membranes (GE Healthcare). The membranes were blocked at room temperature for 1 h using PBS-milk (PBS; 0.1% Tween-20; 5% non-fat dry milk). The membranes were then incubated overnight at 4˚C with rabbit anti-actin antibody (1:1,000; cat. no. A2066; Sigma-Aldrich; Merck KGaA), mouse monoclonal anti-MAD2 (1:500; cat. no. sc-374131; Santa Cruz Biotechnology, Inc.), mouse anti-E-cadherin (1:1,000; cat. no. 14472), mouse anti-N-cadherin (1:1,000; cat. no. 14215), rabbit anti-vimentin (1:1,000; cat. no. 5741) (all Cell Signaling Technology, Inc.) or Apoptosis Western Blot Cocktail (pro/p17-caspase-3, cleaved PARP, muscle actin) (1:400; cat. no. ab136812; Abcam). This cocktail is designed to study the induction of apoptosis in response to various stimuli and includes monoclonal antibodies specific for procaspase-3, caspase-3 and PARP. In particular, the mouse PARP antibody of this cocktail detects only the apoptosis-specific 89-kDa PARP fragment (cleaved PARP). The following day, the membranes were incubated with peroxidase-conjugated anti-rabbit or anti-mouse IgG secondary antibody (both 1:4,000; cat. nos. A6154 and A9044, respectively; both

Sigma-Aldrich; Merck KGaA) for 2 h at room temperature. A UVITEC Alliance LD (Uvitec Ltd.) western blot detection system with SuperSignal Technology reagent (Thermo Fisher Scientific, Inc) and the Alliance 1D Max software (Uvitec Ltd.) was used to visualize the signals.

Colony formation assay. SW1736 and 8505C cells were treated with vehicle (DMSO) or 1.5 μM DHT for 48 h, then seeded at $1.5x10^3$ cells/plate. Colonies were left to form for 21 days, then washed twice with PBS and fixed with pure methanol for 15 min at 4˚C. Cells were then washed twice with PBS-Triton X-0.1% (Sigma-Aldrich; Merck KGaA) and incubated at room temperature with crystal violet (Sigma-Aldrich; Merck KGaA) solution for 30 min. Crystal violet was removed and stained colonies were washed, images were captured and colonies were counted by eye.

Soft agar assay. The clonogenic ability of the SW1736 and 8505C cells after treatment with 1.5 μM DHT was evaluated using a soft agar assay. Briefly, after 48 h of treatment, cells were collected, and $1x10^4$ cells were suspended in 4 ml complete medium containing 0.25% agarose (Sigma-Aldrich), then seeded to the top of a 1% agarose complete medium layer in 6-cm plates. The colonies were counted by eye in four different fields, under a Leica DMI-600B inverted microscope (Leica Microsystems Ltd.). Data are representative of three independent experiments.

Transwell invasion assays. Transwell membranes coated with Matrigel™ were used to measure the ability of cells to attach to the matrix, invade into and through the matrix, and migrate towards a chemoattractant. The invasion ability of ATC cells was evaluated after treatment for 72 h with 1.5 μM DHT. For each cell line, $2.5x10^4$ live cells per condition (DHT or vehicle) were separately re-suspended in culture media containing 10% FBS and seeded in a 24-well plate Transwell coated with Matrigel, as described by Justus *et al* (33). RPMI-1640 medium supplemented with 25% FBS was used as the chemoattractant in the lower chamber. After 24 h, cells were fixed with 70% ethanol and stained with crystal violet solution. After staining, the top of membrane was gently scraped to remove the cells that had not migrated; the cells that had migrated through the membrane toward the chemoattractant were attached on the underside of the membrane. The number of cells on the underside were counted in six different fields of view using an inverted microscope (Leica DMI-600B). Data are representative of the average of the sum of the cells counted in all these six fields in three independent experiments.

High-throughput RNA sequencing and analysis. RNA was extracted from SW1736 and 8505C cells treated with vehicle (DMSO) or DHT using a RNeasy Mini kit (Qiagen GmbH) according to the manufacturer's instructions. In total, ~1 μg RNA (RNA integrity number >7) was used as the starting material for preparation of the library using a Universal Plus mRNA-Seq kit (cat. no. 0520-A01; Tecan Group, Ltd.) according to the manufacturer's protocol. RNA samples were quantified, and the quality was assessed using an Agilent 2100 Bioanalyzer RNA assay (Agilent Technologies, Inc.) and the final libraries were checked using both a Qubit 2.0 Fluorometer (Invitrogen; Thermo Fisher Scientific, Inc.) and Agilent Bioanalyzer DNA assay. The library final concentration was 68.7 nM. Libraries (1.4 nM) were then prepared for sequencing using the single-end 75 bp mode on a NextSeq 500 (Illumina, Inc.). The Bcl2Fastq version 2.20 in the Illumina pipeline was used for processing the raw data (format conversion and de-multiplexing); adapter sequences were masked with Cutadapt version 1.11 (34) from raw fastq data and the ERNE (35) software was used to remove lower quality bases and adapters. Reads were aligned to the reference hg38 genome/transcriptome using STAR software (36). Finally, assembly and quantitation of full-length transcripts representing multiple spliced variants for each gene locus was performed using the Stringtie tool (37). Differentially expressed genes were defined as those with a $\log_2$ fold change >1.5 or <-1.5. Raw and processed data are available on the public online repository Gene Expression Omnibus (dataset no. GSE168616).

Gene expression assays. A total of 500 ng total RNA from SW1736 and 8505, extracted as described above, was reverse transcribed to cDNA using random hexaprimers and SuperScript III (SSIII) reverse transcriptase (Thermo Fisher Scientific, Inc.). Briefly, the first strand cDNA synthesis was created in a total volume of 20 μl with 5X First-strand buffer, DTT 0.1 M, RNase OUT Recombinant RNase Inhibitor (Thermo Fisher Scientific, Inc.), dNTPs 10 mM, random primers (Thermo Fisher Scientific, Inc.) and SSIII reverse transcriptase. The reverse transcription step involved incubation at room temperature for 5 min, 50˚C for 60 min, 70˚C for 15 min and 45˚C for 5 min. Quantitative PCR was performed using PowerUP Sybr green master mix (Thermo Fisher Scientific, Inc.) on the QuantStudio3 system (Applied Biosystems; Thermo Fisher Scientific, Inc.), as previously described (38) and following the Standard cycling mode (primer T_m <60˚C): 50˚C for 2 min, 95˚C for 2 min and 95˚C for 15 sec, 60˚C for 15 sec and 72˚C for 1 min for 40 cycles. The QuantStudio Design and Analysis software (Applied Biosystems; Thermo Fisher Scientific, Inc.), was used to calculate mRNA levels with the $2^{-\Delta\Delta Cq}$ method (39) and β-actin was used as reference. All experiments were performed in triplicate. Oligonucleotide primers were purchased from Sigma-Aldrich; Merck KGaA, and the sequences of the primers are listed in Table I.

Statistical analysis. Data are presented as the mean ± standard deviation. All results were analyzed using the unpaired Student's t-test or one-way ANOVA in GraphPad Prism version 6 (GraphPad Software, Inc.). After one-way ANOVA, the Dunnett's post hoc test was performed. $P<0.05$ was considered to indicate a statistically significant difference.

Results

Effects of DHT on cell viability, cell cycle progression and apoptosis. In the first set of experiments, the effects of DHT on two human ATC cell lines (SW1736 and 8505C) were evaluated. To assess the effects of DHT on cell viability using several doses of DHT, an MTT assay was performed on ATC cells treated for 24, 48 or 72 h. As shown in Fig. 1A, 2 and 3 μM DHT treatment significantly reduced the viability

Table I. Reverse transcription-quantitative PCR primer sequences.

Gene	Forward primer sequence, 5'-3'	Reverse primer sequence, 5'-3'
CDH1	AGCCTCAGGTCATAAACATCATTG	CTCGCCCCGTGTGTTAGTTC
CDH2	CCATCACTCGGCTTAATGGT	ACCCACAATCCTGTTCCACAT
VIM	CAAATCGATGTGGATGTTTCCA	AGGTTCTTGGCAGCCACACT
TWIST1	GCAGGACGTGTCCAGCTC	CTGGCTCTTCCTCGCTGTT
ZEB1	TCAGTGTTCTTCACCGTCTCTTTC	GTTTATTCTCTATCTTTTGCCGTATCTG
ZEB2	CAAGAGGCGCAAACAAGC	GGTTGGCAATACCGTCATCC
ACTB	TTGTTACAGGAAGTCCCTTGCC	ATGCTATCACCTCCCCTGTGTG

CDH, cadherin; VIM, vimentin; ZEB, zinc finger E-box binding homeobox; ACTB, β-actin.

of both ATC cell lines at all time points. In SW1736 cells, doses <2 μM did not significantly affect viability, whereas the 8505C cells were more sensitive to DHT treatment, since they exhibited a ~50% reduction in cell viability when treated with 0.5 and 1 μM DHT after 48 h. However, the effects of DHT were transient, and cell viability recovered at the 72-h time point. Based on these data, the median ED_{50} of 1.5 μM was selected for treatment of both cell lines in subsequent experiments.

The aforementioned experiments did not distinguish whether the reduced viability was the effect of a decrease in cell metabolism or cell number. To evaluate the effects of DHT on cell cycle progression, flow cytometry analysis was performed after 72 h of DHT treatment. As shown in Fig. 1B and C, treated SW1736 and 8505C cells exhibited a slight reduction in the proportion of cells in the G_0/G_1 phase compared with vehicle-treated cells, significative only in SW1736 cells. By contrast, DHT treatment resulted in a significant increase in the proportion of cells in the S phase from 25.8 to 32.3% and from 43.2 to 55.3% in SW1736 and 8505C cells, respectively. Moreover, 8505C treated cells showed a significant reduction in the proportion of cells in the G_2/M. The notable increase in cells with reduced DNA staining compared with G_0/G_1 cells among treated cells was hypothesized to reflect an increase in the degree of apoptosis, as previously described (40).

To evaluate whether the decrease in cell viability observed after the treatments was due to apoptotic cell death, western blot analysis of caspase-3 activation (Fig. 2A and B) and cleaved-PARP protein (Fig. 2C-F) was performed. Caspase-3 activation was evaluated after 24 and 48 h of treatment with 0.75 or 1.5 μM DHT. In both cell lines, 48-h treatment with 1.5 μM DHT resulted in a significant increase in caspase-3 activation compared with the DMSO control. These conditions also resulted in a ~60-fold increase in the expression of cleaved-PARP levels compared with the control in both cell lines (Fig. 2E and F).

To better characterize the effects of DHT on cell death, an Annexin V/propidium iodide assay was performed. As shown in Fig. 2G, in both cell lines, 1.5 μM DHT treatment resulted in an increase in the proportion of necrotic (top left area of the plot) and late apoptotic cells (top right area of the plot).

Effects of DHT on cell colony forming ability and invasiveness. To assess the effects of DHT on markers of aggressiveness in the two ATC cells, its influence on the ability of cells to form colonies in an anchorage-dependent or independent manner was assessed using a plate colony formation assay and a soft-agar colony formation assay. As shown in Fig. 3A and B, there was a significant reduction in the number of colonies in cells treated with 1.5 μM DHT. In 8505C cells, DHT reduced the number of colonies by ~10-fold, and its effects were more potent on the SW1736 cells, in which it completely abrogated colony formation ability. To better evaluate the effects of DHT on tumor cell aggressiveness, the anchorage-independent colony formation ability of SW1736 and 8505C treated with DHT was investigated by performing a soft agar colony formation assay. Treatment with 1.5 μM DHT for 48 h resulted in a significant reduction in the number of colonies in both cell lines relative to the respective vehicle-treated cells (Fig. 3C and D).

Since traversing the basement membrane by cancer cells is an important step in the metastatic process, the effects of DHT treatment on thyroid cancer cell invasiveness was assessed using Transwell invasion assays. Treatment with 1.5 μM DHT resulted in a significant decrease in cell invasion in both ATC cell lines (Fig. 3E and F).

Effects of DHT on gene expression. To evaluate the effects of DHT on gene expression, high-throughput RNA-seq analysis was performed on the SW1736 and 8505C cells treated with 1.5 μM DHT for 24 h. After filtering out low quality reads, the comparison between cells treated with DMSO or DHT showed that 1,805 and 503 genes were differentially expressed (log_2 fold change >1.5) in the DHT-treated SW1736 and 8505C cells, respectively. In SW1736 cells, 813 genes were upregulated and 992 were downregulated, whereas in 8505C, 350 genes were upregulated and 153 were downregulated in response to DHT treatment. Among these, 41 genes were commonly upregulated and 29 commonly downregulated (Fig. 4).

Gene Ontology analysis was then performed using the Panther Classification System (41). Briefly, differential expressed gene lists for each cell line (separately for up- and down-regulated genes) were loaded into PANTHER (version 16.0) and mapped to its pathway database. When the PANTHER pathway database was interrogated with the commonly dysregulated genes, no pathway has been identified as significantly deregulated. Regarding the altered genes in each cell line, the top 10 up- and downregulated pathways of

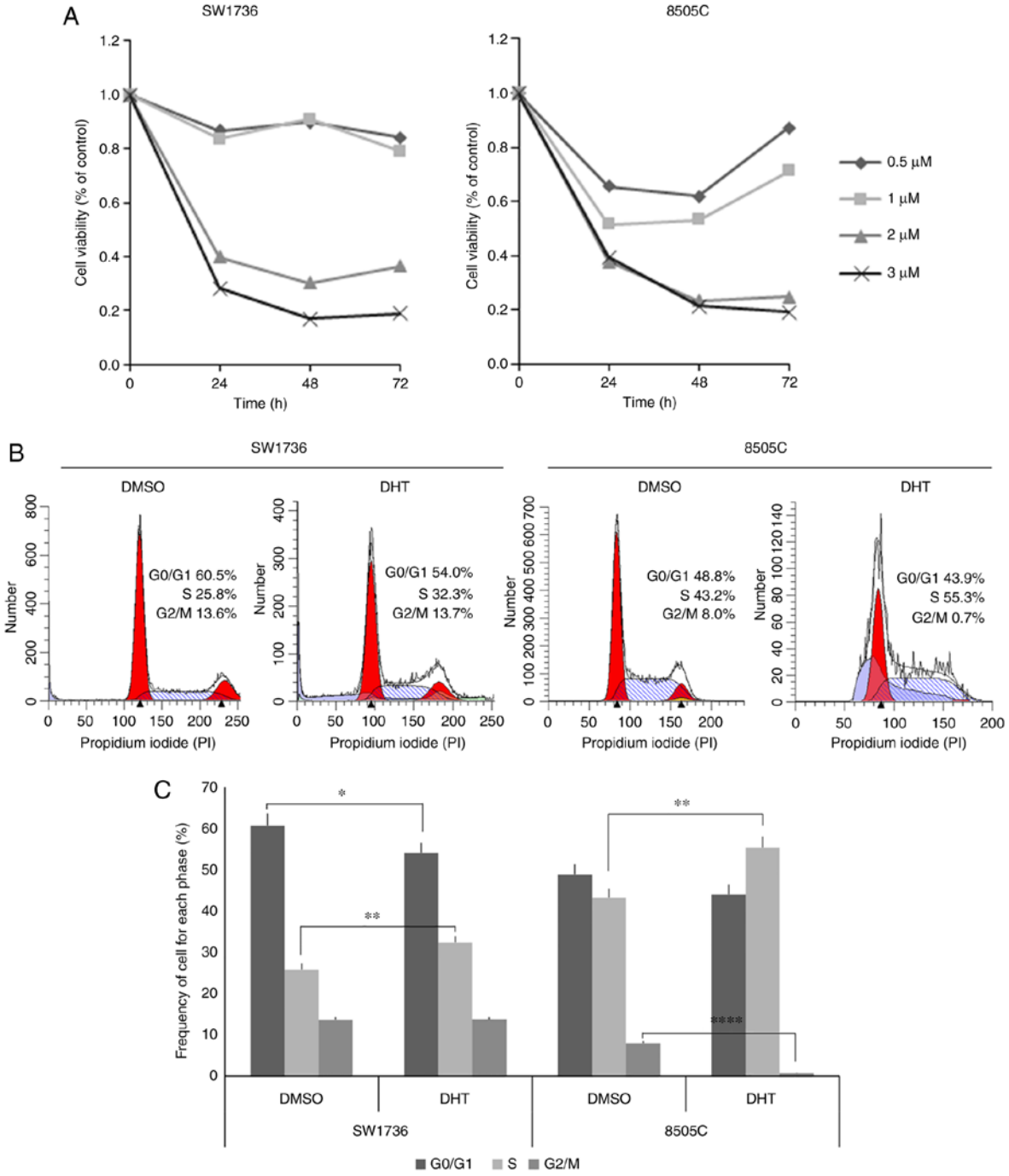

Figure 1. DHT affects thyroid cancer cell viability and cell cycle progression. (A) SW1736 and 8505C cells were treated with DHT at different doses (rising from 0.5 to 3 μM) or vehicle (DMSO) for 24, 48 or 72 h, and cell viability was analyzed using MTT assays. Each point represents the mean of six measurements. (B) Cell cycle analysis of SW1736 and 8505C cells treated with DMSO or 1.5 μM DHT for 48 h. (C) Histogram of the cell cycle analysis of SW1736 and 8505C cells. n=3. *P<0.05, **P<0.01, ****P<0.0001; Student's t-test. DHT, dihydrotanshinone.

each cell line are shown in Fig. 5 (and Tables SI-IV). Although the altered gene expression involved different genes, the analysis identified some commonly dysregulated pathways in both cell lines, which included 'Wnt signaling' (P00057), 'apoptosis signaling' (P00006) and 'cadherin signaling pathway' (P00012).

Effects of DHT on expression of EMT markers. To characterize the effects of DHT on ATC cell aggressiveness at the molecular level, the expression of five universally recognized genes associated with EMT (42), a phenotypic change which endows cancer cells with increased migratory and invasive capacity, was analyzed.

The changes in mRNA levels for the EMT-related genes *CDH1, CDH2, VIM, TWIST, ZEB1* and *ZEB2* are shown in Fig. 6A. Treatment with 1.5 μM DHT resulted in a significant increase in the expression of *CDH1*, a marker of the epithelial phenotype, in treated cells compared with those treated with DMSO. Additionally, DHT treatment significantly decreased the gene expression levels of all other markers, which are associated with the mesenchymal phenotype, in both cell lines, except for *CDH2*, confirming that DHT modulated EMT.

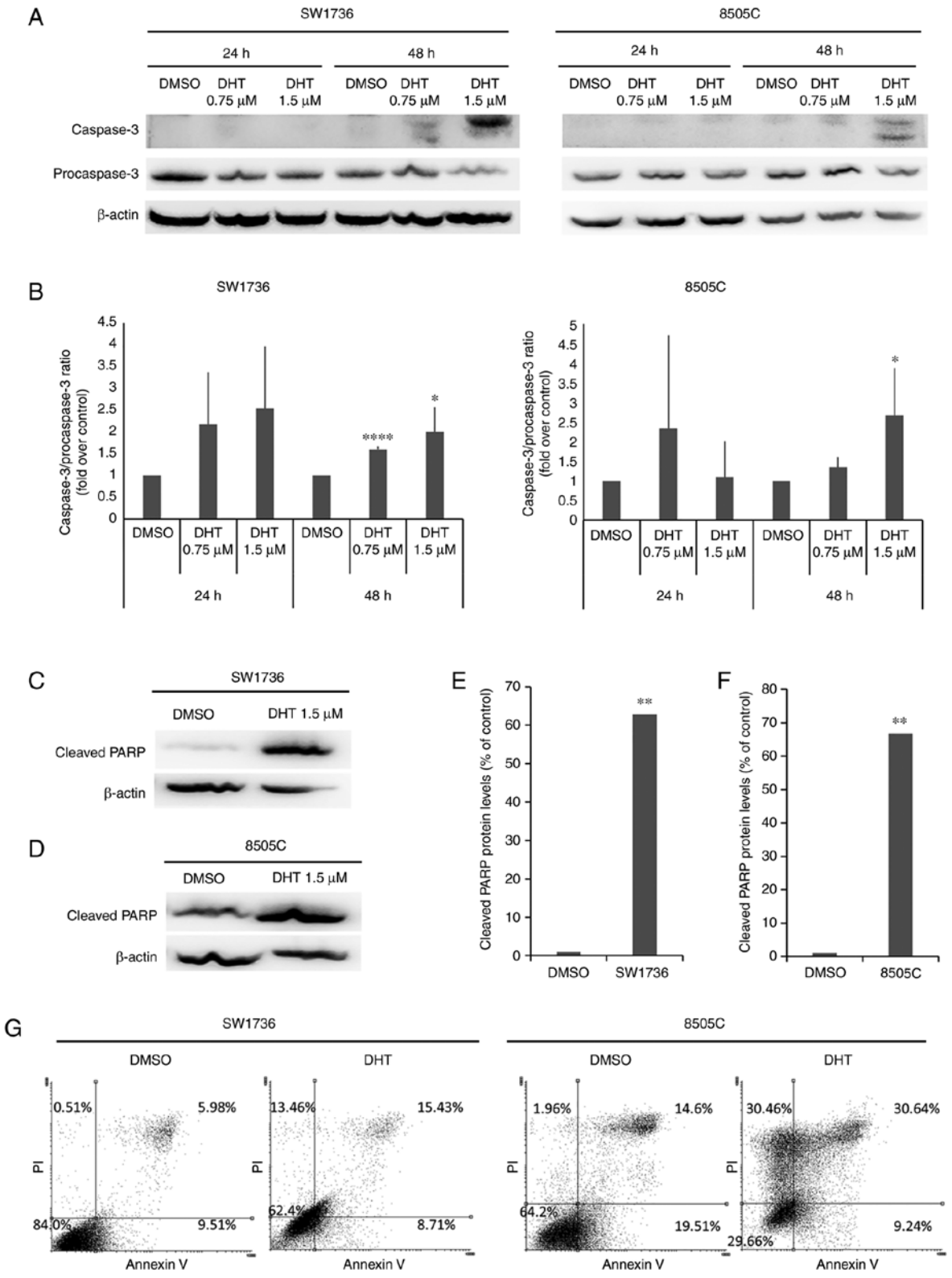

Figure 2. DHT affects thyroid cancer cell death. (A) Protein expression levels of cleaved caspase-3, procaspase-3 and β-actin in SW1736 and 8505C cells treated with DMSO or DHT 1.5 μM for 48 h. (B) Densitometric analysis of cleaved caspase-3 and procaspase-3 levels normalized against β-actin. (C and D) Protein expression levels of PARP and β-actin in SW1736 and 8505C cells treated with DMSO or DHT 1.5 μM for 48 h. (E-F) Densitometric analysis of cleaved PARP levels obtained with Western Blot assay normalized against β-actin. For each cell line, the results are expressed as percentage over control. (G) Annexin V and propidium iodide staining of SW1736 and 8505C cells treated with DMSO or DHT 1.5 μM for 48 h. n=3. *P<0.05, **P<0.01, ****P<0.0001; Student's t-test. DHT, dihydrotanshinone.

Among the EMT-related genes assessed, *CDH1*, *CDH2* and *VIM* are particularly interesting, as they are phenotypic markers of EMT. Thus, their protein expression levels were also assessed. VIM and CDH2 protein expression levels were significatively reduced following treatment with DHT (Fig. 6B and C). Despite the fact that CDH1 mRNA levels

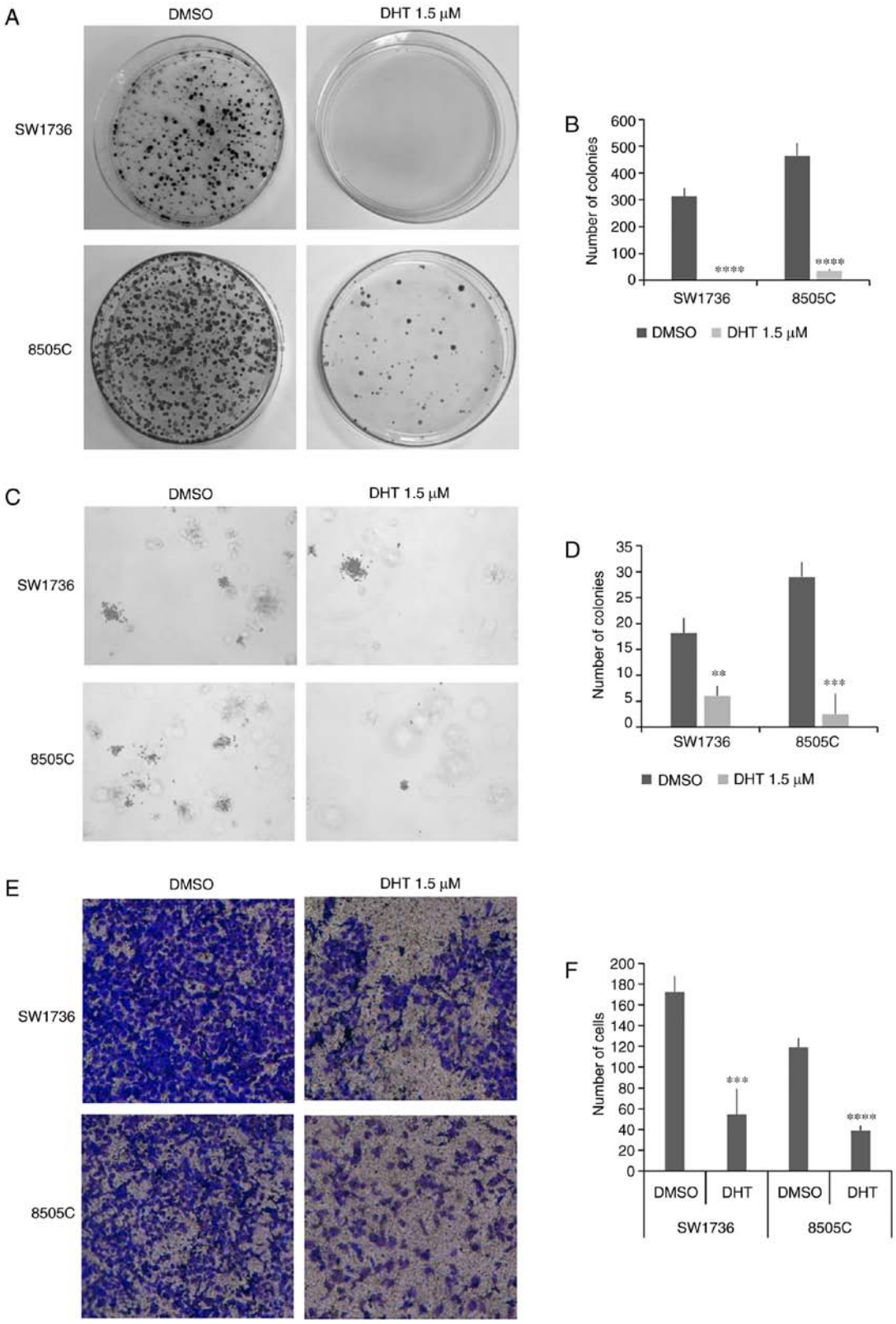

Figure 3. DHT affects the colony formation ability and invasiveness of ATC cells. (A) Colony formation in SW1736 and 8505C cells treated with 1.5 μM DHT or vehicle (DMSO) for 48 h. (B) Representative bar chart of the number of colonies after 21 days. (C) Tumor aggressiveness was evaluated as the clonogenic ability of ATC cells using a soft-agar assay. Magnification, x4. (D) Bar chart represents the number of colonies in each line after the treatments. (E) Tumor invasiveness was evaluated 72 h after treatment. Magnification, x10. (F) Invasiveness (number of counted cells per field) of each cell line treated either with DHT or DMSO for 72 h. n=3. **P<0.01, ***P<0.001, ****P<0.0001; Student's t-test. DHT, dihydrotanshinone; ATC, anaplastic thyroid cancer.

were increased following DHT treatment, the protein expression levels remained undetectable in the treated cells (data not shown).

Effects of DHT on MAD2 expression. Since DHT is known to inhibit the activity of the RNA-binding protein HuR (24), to verify the involvement of HuR in the effects of DHT on

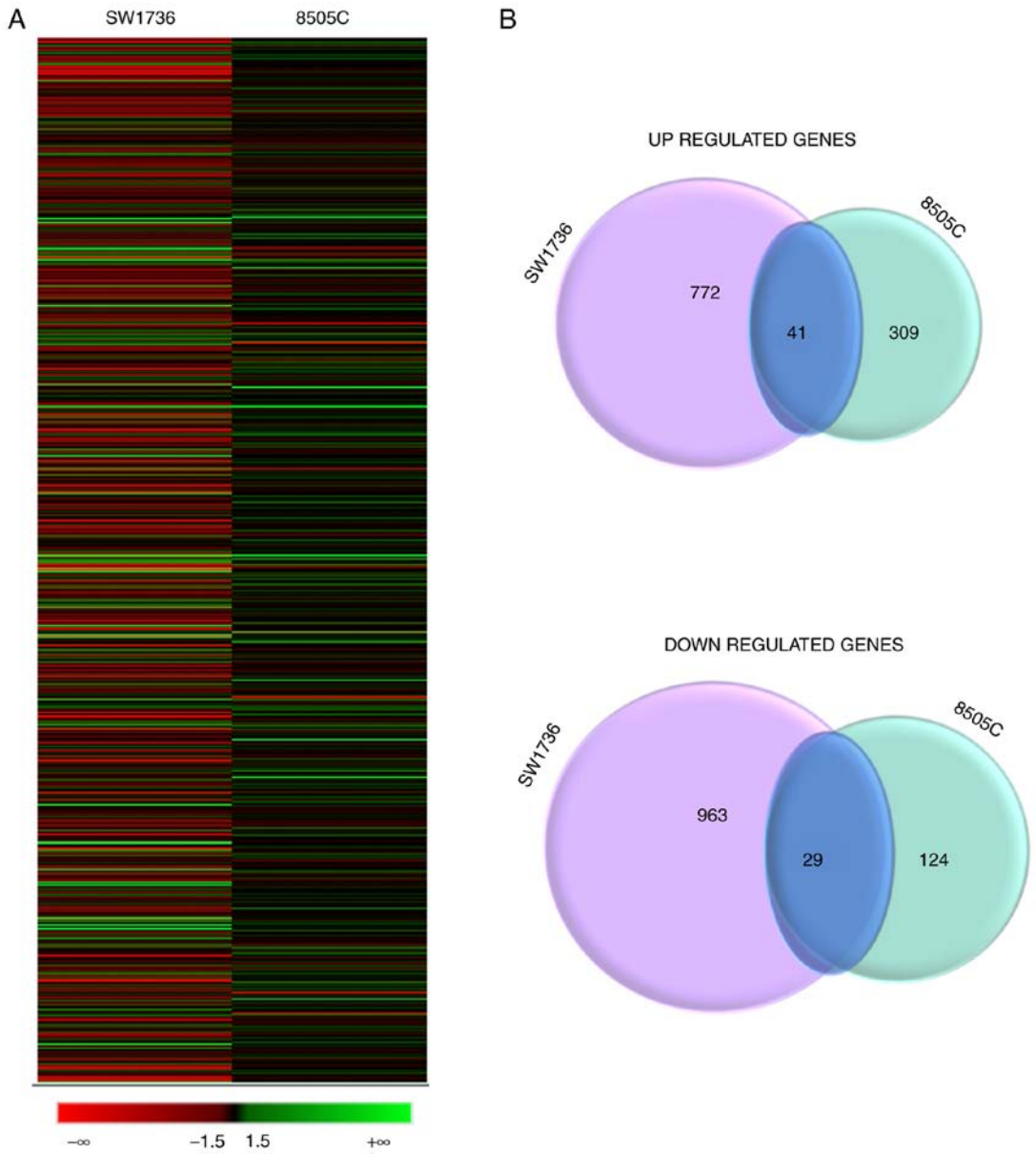

Figure 4. DHT effects on gene expression. (A) Heat maps showing the hierarchical clustering of mRNA in SW1736 and 8505C cell lines. Cells were treated either with DHT or vehicle for 72 h. Results are showed as Fold Change (Log2). (B) Venn diagrams represented the comparison of up-regulated, down-regulated between SW1736 and 8505C cell lines after RNA-seq data analysis. Light blue gene clusters indicated shared modified genes between the two cell lines.

viability, apoptosis and tumor aggressiveness in ATC cells, MAD2, a target of HuR, was then analyzed. MAD2, which is one of the major factors involved in the spindle checkpoint, has been shown to be implicated in cancer progression (43,44) and is overexpressed in thyroid neoplasms (45). Thus, the effects of DHT on MAD2 protein expression were examined using western blotting (Fig. 7). After 48 h of treatment with 1.5 μM DHT, there was a significant decrease in MAD2 protein expression levels in both cell lines. This result demonstrated that MAD2 may be involved in anticancer effect of DHT in ATC cell lines.

DHT administration increases the sensitivity of ATC cells to cisplatin treatment. Based on the results of the DHT treatment, the effects of its co-administration with cisplatin, one of the few chemotherapeutic agents used for ATC treatment, were then examined. The effect of their combined administration on the viability of SW1736 and 8505C cells was assessed following 24, 48 or 72-h treatment with cisplatin and DHT alone or combined. Since synergy is considered as the interaction between two or more drugs, which results in a total effect of the drugs, which is greater than the sum of the individual effects of each compound, drug concentrations of 1 μM for both compounds were used, as this concentration did not exert any notable effects when the compounds were administered alone.

As shown in Fig. 8, DHT and cisplatin 1 μM alone did not affect cell viability after 72-h treatment, in either cell line. However, when co-administered at the same individual concentration of 1 μM, there was a significant decrease in cell viability of around 60-70% in both the SW1736 and 8505C cells.

Thus, the effects of DHT-cisplatin combination on apoptosis and other markers of tumor aggressiveness were assessed next (Fig. 9). Western blot analysis indicated that cleaved

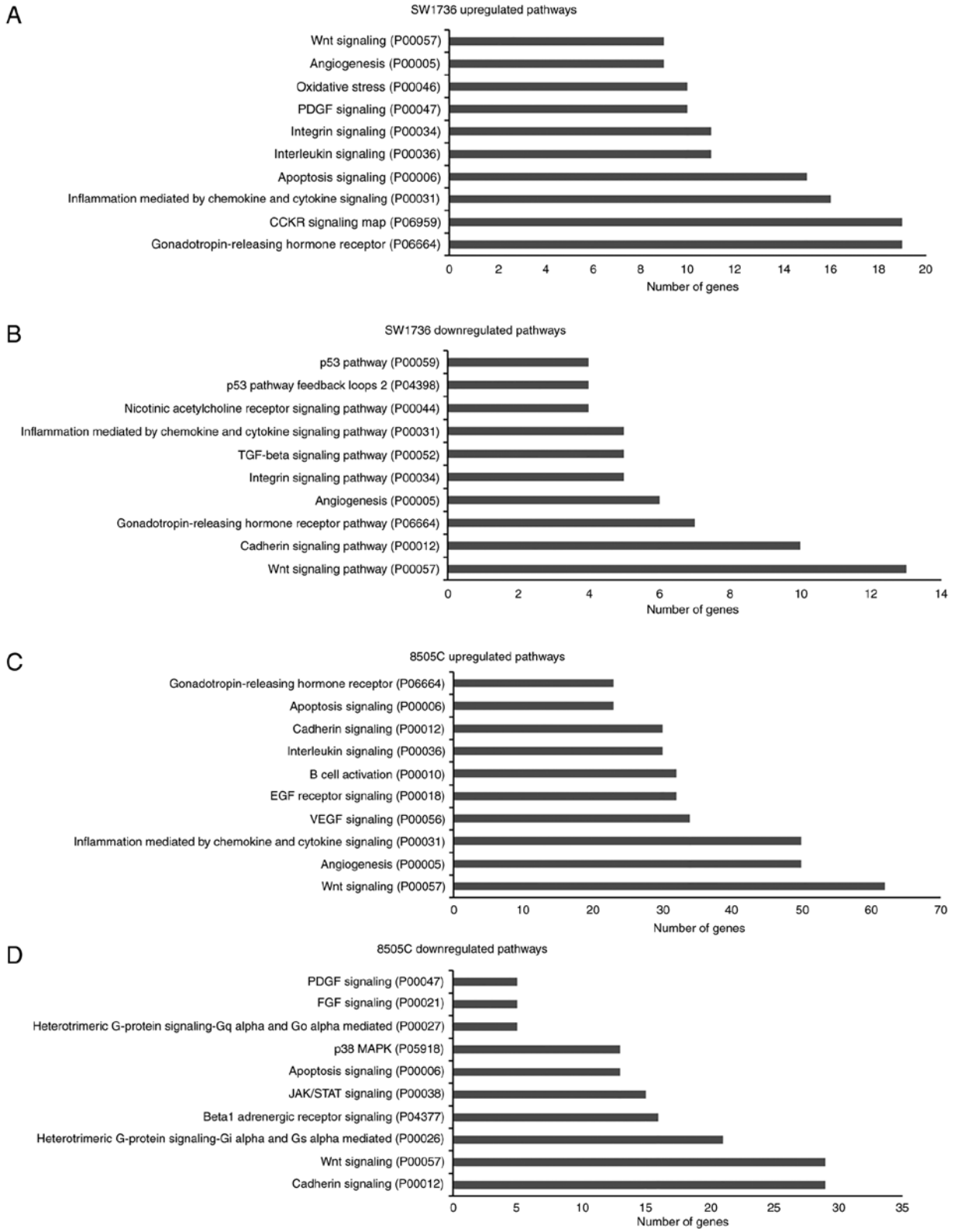

Figure 5. Top 10 deregulated pathways. (A and B) Top 10 (A) upregulated and (B) downregulated pathways in SW1736 treated with DHT 1.5 μM. (C and D) Top 10 (C) upregulated and (D) downregulated pathways in 8505C treated with DHT 1.5 μM. Pathway analysis was performed using the Panther classification system. DHT, dihydrotanshinone.

PARP protein levels were increased 6-fold after cotreatment compared with 1 μM cisplatin alone in SW1736 cells. In 8505C cells, combined administration of DHT and cisplatin resulted in a significant increase in cleaved-PARP protein expression compared with either treatment alone. Similar to what was observed when DHT was used at an ED_{50} dose, the lower dose of 1 μM resulted in MAD2 downregulation in the ATC cell lines. Moreover, cotreatment resulted in a greater decrease in MAD2 protein expression in the SW1736 and 8505C cells, compared with DHT or cisplatin alone.

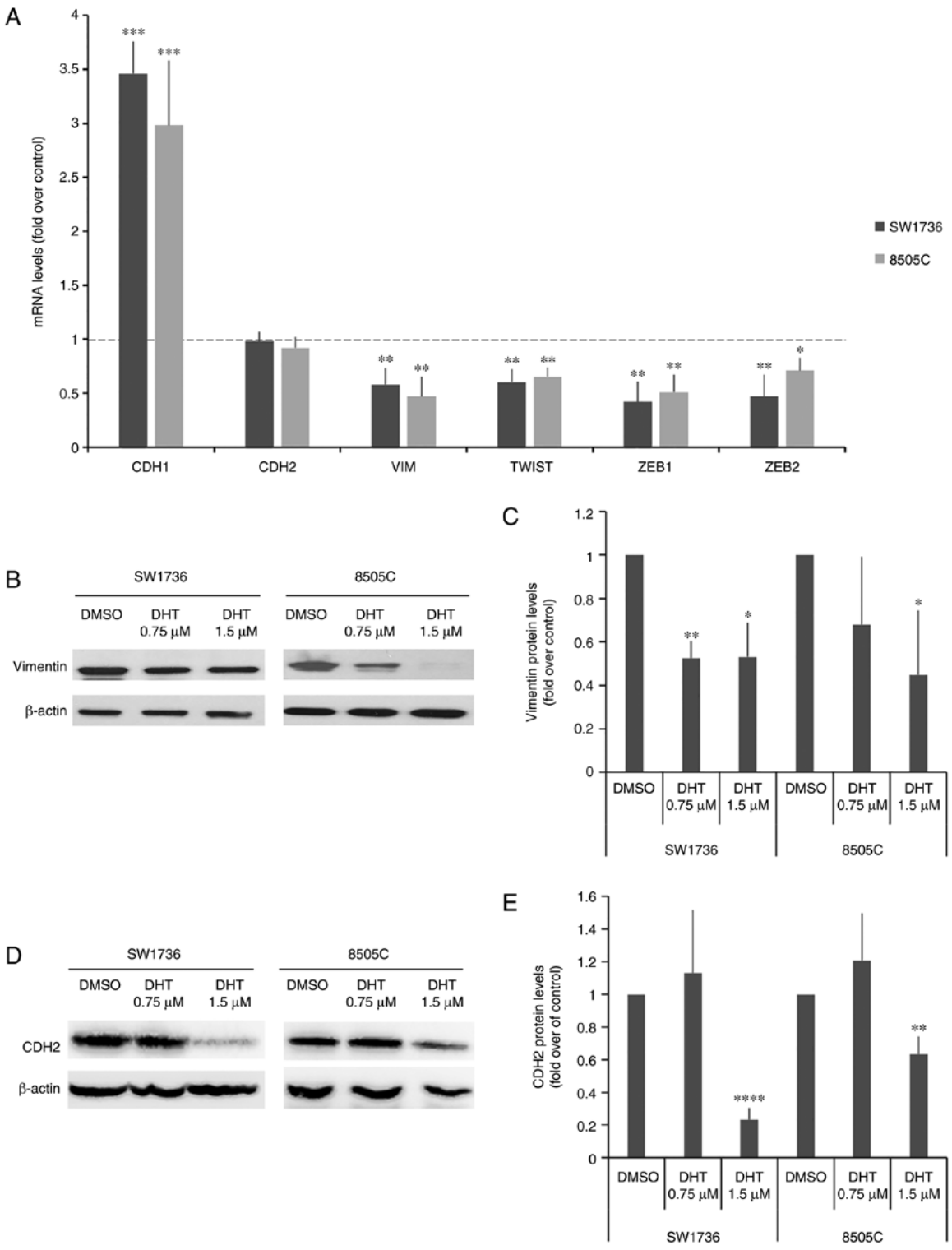

Figure 6. DHT affects EMT-related gene expression in anaplastic thyroid cancer cells. (A) Relative expression levels of EMT-related genes mRNA following 1.5 μM DHT treatment for 48 h. Data are normalized against β-actin levels. (B) Vimentin protein expression levels in SW1736 and 8505C cells treated with DMSO or 0.75 μM or 1.5 μM DHT for 48 h. (C) Densitometric analysis of vimentin protein levels in cells treated with 1.5 μM DHT or DMSO. Data are normalized against β-actin levels. (D) CDH2 protein expression levels in SW1736 and 8505C cells treated with DMSO or 0.75 or 1.5 μM DHT for 48 h. (E) Densitometric analysis of CDH2 protein levels in cells treated with 1.5 μM DHT or DMSO. n=3. *P<0.05, **P<0.01, ***P<0.001, ****P<0.0001; Student's t-test. DHT, dihydrotanshinone; CDH2, cadherin 2.

The effects of the combination of the two compounds on the expression of EMT-related genes were then evaluated. During EMT, CDH1 expression is significantly decreased, whereas CDH2 expression is increased. Thus, CDH2/CDH1 expression ratio is widely considered a marker of EMT (46). As shown in Fig. 10, in SW1736 cells, DHT alone did not induce an increase in the *CDH2/CDH1* ratio, whereas cisplatin, alone and combined with DHT, resulted in a significant reduction in the CHD2/CDH1 ratio. In SW1736, unlike what observed using the ED_{50} dose of DHT (1.5 μM), treatment with 1 μM

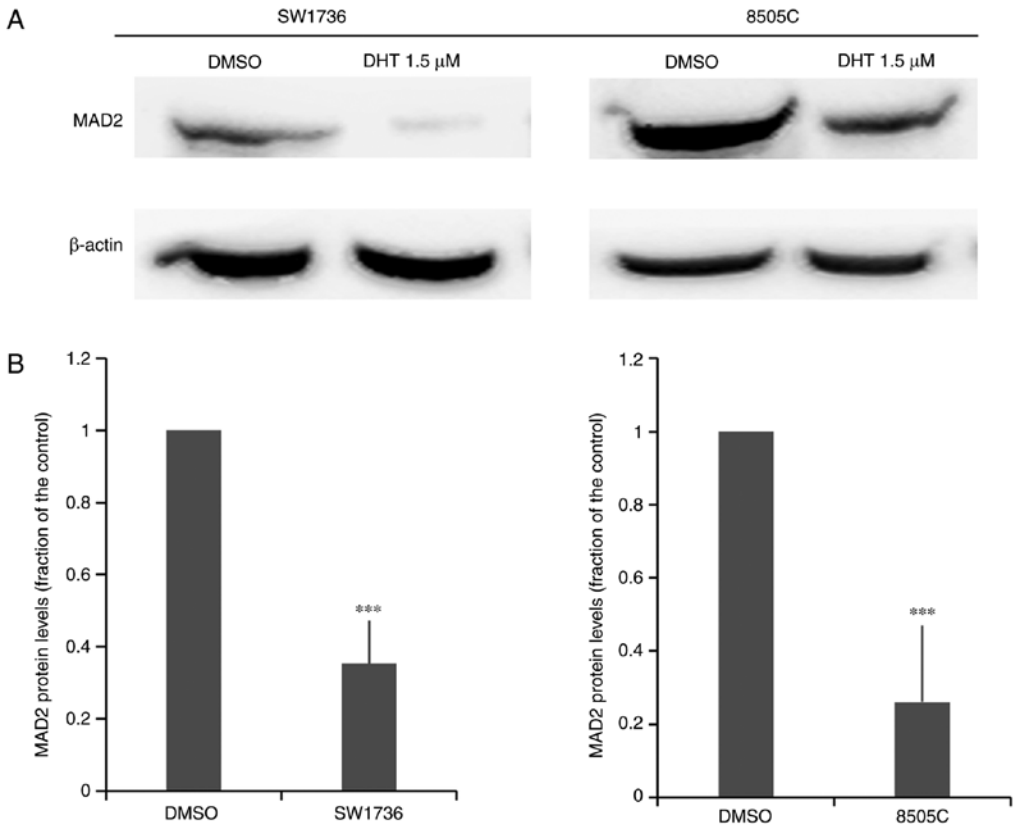

Figure 7. DHT affects MAD2 protein expression. (A) MAD2 protein expression levels in SW1736 and 8505C cells treated with DMSO or 1.5 μM DHT for 48 h. (B) Densitometric analysis of MAD2 protein levels in SW1736 and 8505C cells. Data are normalized against β-actin levels. ***P<0.001; Student's t-test. DHT, dihydrotanshinone.

DHT resulted in an increase in *VIM* mRNA expression levels, compared with the control. When cells were cotreated with DHT and cisplatin, the mRNA expression of *VIM* returns to comparable levels with control, while *ZEB1* decreased. In the 8505C cells, the observed effects on EMT-related genes were not as prominent and the differences were not significant.

Discussion

The post-diagnosis survival rate of ATC is <1 year due to its invasiveness and frequent metastasis, making it the most lethal thyroid malignancy (47). A study of Fan *et al* (48) has focused on different trimodal treatment regimens, namely aggressive radiotherapy in combination with surgery and systemic therapy, but the prognosis of patients with ATC remains poor despite the use of these aggressive multimodal therapies. For these reasons, the search for novel approaches to the treatment of this aggressive thyroid cancer is crucial, as it cannot be effectively managed by the currently available therapies (49). Novel strategies can take advantage of the molecular alterations that occur in these tumors (50). Promising results have been observed in clinical trials of targeted therapy in ATC (50), underscoring the importance of a selection of patients based on tumor molecular profiles. Additional studies are focusing on the use of bioactive molecules that are naturally present in plants, such as phytochemicals, some of which are able to regulate certain cell physiological pathways, which may promote malignant transformation or drug resistance (51,52). Indeed, several studies have reported the anticancer proprieties of several phytochemicals, including some acting on ATC cells (12,13). Moreover, there are natural compounds that may also improve cancer sensitivity to commonly used chemotherapeutic agents (53,54). The lack of effective and standardized therapeutic strategy for the management of ATC, and the promising anticancer effects obtained in preclinical experimental models by certain phytochemicals, highlight them as ideal candidates for investigation as ATC treatments. Several studies have investigated the use of phytochemicals for the treatment of ATC. For instance, Schwertheim *et al* (55) and Allegri *et al* (56) independently demonstrated the antitumoral effects of curcumin, as well as other phytochemicals, in different ATC cells.

In the present study, the effects of DHT were examined. DHT is one of 40 tanshinones extracted from *Salvia miltiorrhiza,* which not only has anticancer activity through its cytotoxic properties, but also improves the sensitivity to other anti-cancer agents drugs and exhibits synergism with other chemotherapeutic regimens (15). Interestingly, DHT has been shown to induce cell death via autophagy in multidrug-resistant colon cancer cells (57) and to enhance irradiation-induced cytotoxic effects, G_2-phase arrest and apoptosis in HeLa cells (23). Moreover, DHT was able to sensitize tumors to irradiation *in vivo* (23). In the present study, it was demonstrated for the first time that DHT exerts strong anticancer activity against ATC cells. Indeed, a decrease in ATC cell viability was observed, which was primarily due to the activation of the apoptotic process, as indicated by a large increase in the cleaved-PARP fraction. Moreover, cell

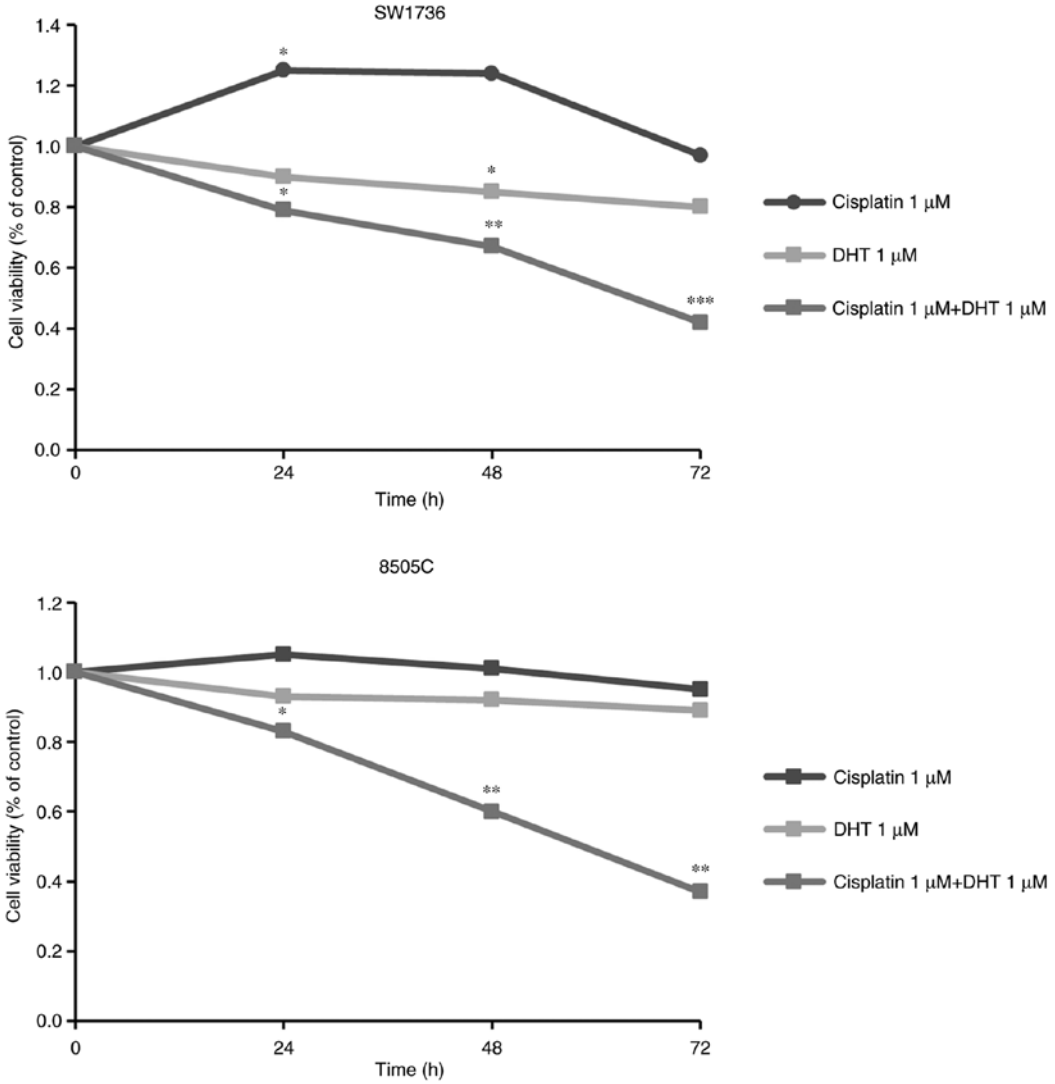

Figure 8. Effects of DHT and cisplatin cotreatment on anaplastic thyroid cancer cell viability. SW1736 and 8505C cells were treated with 1 μM cisplatin or DHT alone, with 1 μM cisplatin 1 and 1 μM DHT or with vehicle (DMSO) for 24, 48 or 72 h. Cell viability was analyzed using MTT assays. Each point represents the mean of six measurements. *P<0.05, **P<0.01, ***P<0.001 vs. control; one-way ANOVA. DHT, dihydrotanshinone.

cycle analysis demonstrated that DHT induced S-phase arrest of ATC cells, which has already been shown in other cancer models (17). The calculated DHT ED_{50} in SW1736 and 8505C cells was almost 50-fold lower than those of others phytochemicals (56), highlighting the effectiveness of its antitumor function in these cell lines.

The molecular mechanisms regulated by DHT remain to fully elucidated. Tan *et al* (58) demonstrated that DHT inhibits glioma cell proliferation through the activation of ferroptosis, regulating the expression of *ACSL4* and the *GPX* gene family. Moreover, Wang *et al* (59) showed that DHT transcriptionally repressed *PIK3CA*. These studies suggest that DHT primarily exerts its functions by regulating gene expression. Thus, in the present study, the effects of DHT on gene expression were evaluated using high-throughput RNA-sequencing analysis on SW1736 and 8505C cells. Despite the differences in the altered expression of genes, the analysis identified certain commonly dysregulated pathways, including the Wnt, apoptotic and cadherin signaling pathways.

These encouraging results obtained with regard to cell viability and apoptosis are strengthened by those obtained with regard to counteracting other features of aggressive tumor behavior, as the invasiveness of a few aggressive cells that survive can lead to dissemination and re-growth of metastasizing tumor cells. In this context, the effects of DHT on several features of tumor cell aggressiveness were analyzed by performing colony formation, soft agar and invasion assays, whilst also determining the expression of EMT-related genes. DHT significantly reduced the colony formation ability of ATC cell lines, achieving complete inhibition of colony formation of SW1736 cells. Moreover, DHT treatment significantly reduced invasiveness of ATC cells, indicating that this compound can affect mesenchymal motility. This latter property was also confirmed by the effects obtained by analyzing the effects on some key elements of the EMT process, which is typical of aggressive neoplasia. Indeed, DHT treatment resulted in an increase in *CDH1* expression and a significant decrease in *VIM, TWIST, ZEB1* and *ZEB2* expression (components of the cytoskeleton, the extracellular matrix or transcription factors), which are considered the five key EMT-related genes (40). Our findings showed that DHT regulated the mRNA levels of these

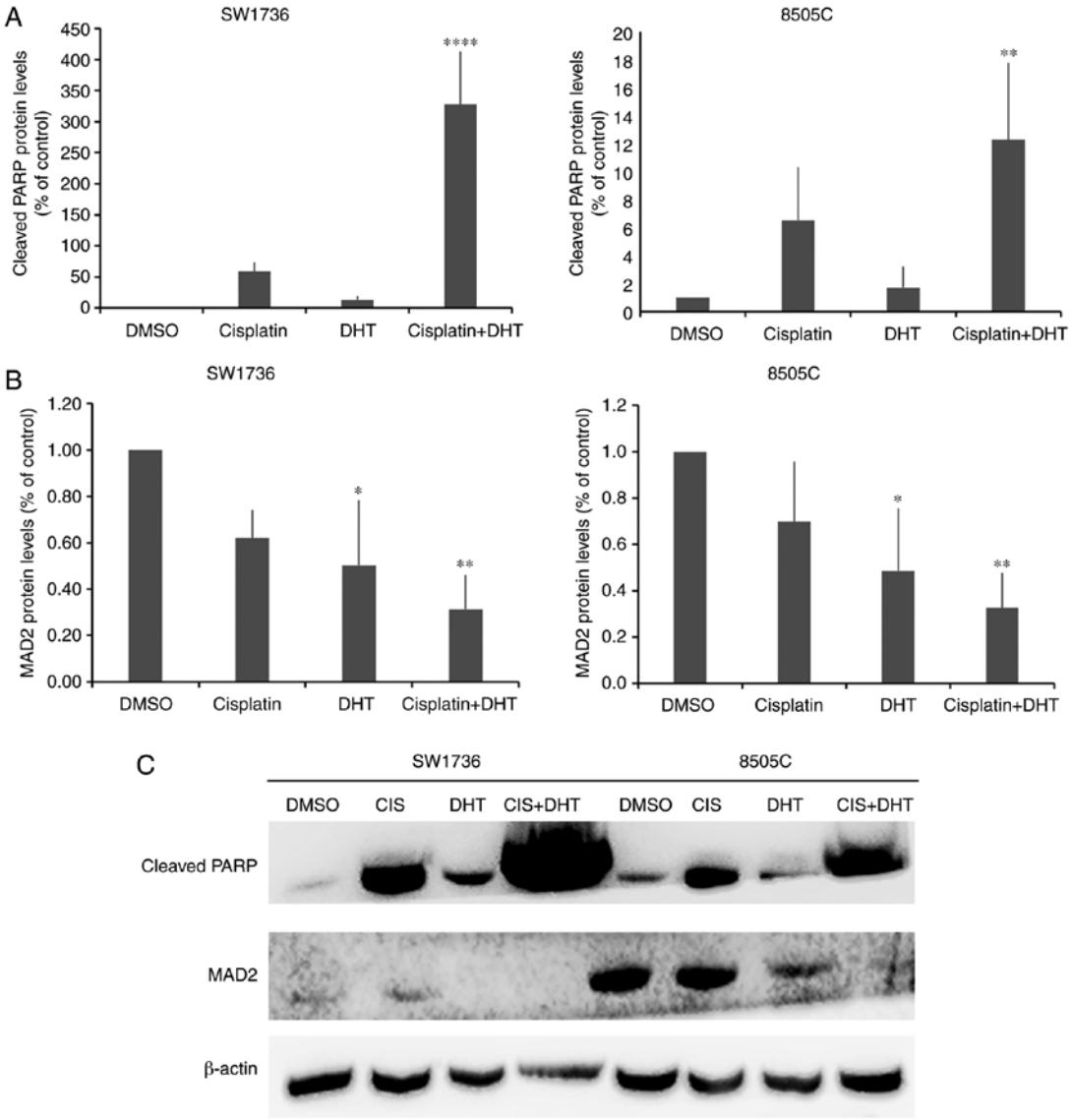

Figure 9. Effects of DHT and cisplatin cotreatment on apoptosis. SW1736 and 8505C cells were treated with 1 μM cisplatin or DHT alone, with 1 μM cisplatin 1 and 1 μM DHT or with vehicle (DMSO) for 48 h. (A and B) Densitometric analysis of (A) cleaved PARP or (B) MAD2 protein levels. Data are normalized against β-actin and expressed as percentage over control. *P<0.05, **P<0.01, ****P<0.0001 vs. control; one-way ANOVA. (C) Representative western blot images. n=3. DHT, dihydrotanshinone; CIS, cisplatin.

genes. Thus, in order to deepen our understanding of the molecular mechanism underlying the effects of DHT, a second phase of our study was performed based on a recent study by Lal *et al* (24), showing that DHT may alter the activity of the RNA-binding protein HuR by inhibiting the HuR-mRNA binding in xenograft tumors. In our previous study, the RNA-binding protein HuR was overexpressed in thyroid cancer, and that its downregulation resulted in anti-cancer effects in ATC cell lines (25-27). Moreover, we also previously showed that a HuR-specific inhibitor (CMLD-2) exerted antitumor effects on ATC cells via downregulation of *MAD2* (25-27). In the present study, DHT may have exerted its antitumor effects, at least partly, by decreasing the expression of the HuR target, MAD2, a protein closely associated with ATC cell viability, survival and aggressiveness (27). Bates *et al* (60) and Pajuelo-Lozano *et al* (61) demonstrated that MAD2 silencing results in reduced tumor aggressiveness and alteration of several biological processes including EMT, in different cancer types. Further experiments focused on the molecular mechanism between MAD2 and EMT induction in thyroid cancer could better highlight the role of MAD2 in thyroid cancer and EMT processes. Furthermore, evaluating whether the effects of DHT are maintained after knockdown of MAD2 would be an interesting experiment.

Nascimento *et al* (62) demonstrated that the combination of MAD2 knockdown with cisplatin administration constituted an efficient approach to the treatment of drug-resistant tumors. Since the present findings indicated that DHT resulted in downregulation of MAD2, the final part of this study was dedicated to the investigation of a synergistic effect between DHT and cisplatin. Seto *et al* (63) reported that cisplatin was able to inhibit ATC progression and improved survival outcomes of certain ATC patients. However, another study demonstrated that cisplatin could activate autophagy-mediated apoptosis resistance (64). Moreover, chemotherapy resistance currently remains a

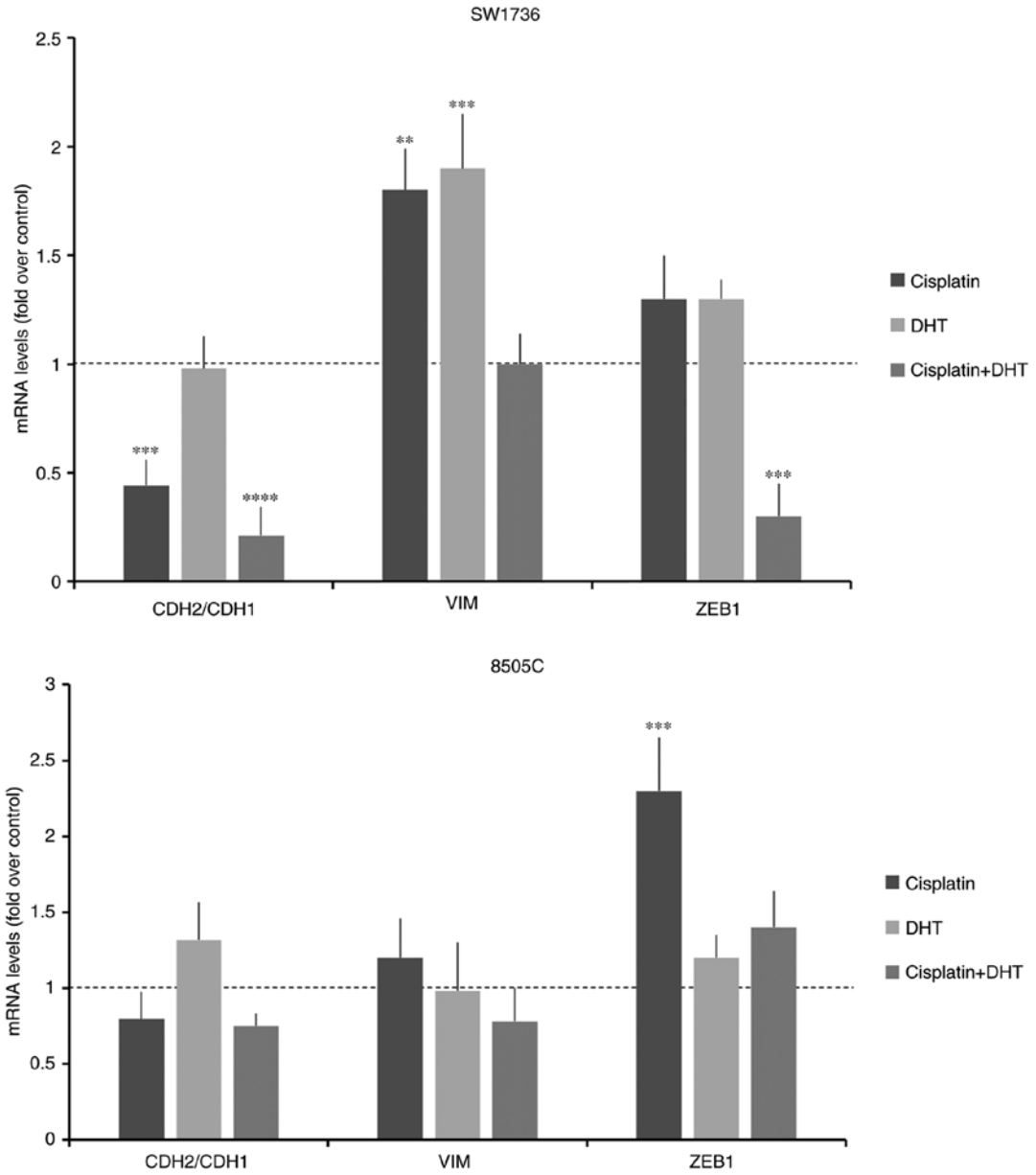

Figure 10. Effects of DHT and cisplatin cotreatment on the expression of EMT-related genes. Relative mRNA expression levels of EMT-related genes in SW1736 or 8505C cells treated with 1 μM cisplatin, 1 μM DHT or 1 μM cisplatin + 1 μM DHT treatment for 48 h. Data are normalized against β-actin levels. **P<0.01, ***P<0.001, ****P<0.0001 vs. control; one-way ANOVA. DHT, dihydrotanshinone; CDH, cadherin; VIM, vimentin; ZEB, zinc finger E-box binding homeobox.

significant hurdle in ATC management (64). Recently, a synergistic effect was demonstrated in thyroid cancer cells cotreated with the phytochemical quercetin and a protein kinase inhibitor (65). In the present study, DHT exerted a synergistic effect with cisplatin, indicating the potential benefits of the use of DHT as an adjuvant in a multimodal therapeutic strategy, in order to improve the antitumor effectiveness of other therapies. An important point regarding these proposed compounds as anticancer drugs is the absence/tolerance of toxicity on normal cells. In this regard, no toxic effects have been reported when DHT is administered for the treatment of xenograft tumors *in vivo* (20,21). Moreover, the possibility of a toxic effect on normal thyroid cells can be excluded in patients with ATC, since the use of anticancer drugs is complementary to the surgical treatment to achieve total thyroidectomy.

In conclusion, to the best of our knowledge, the results of the present study were the first to demonstrate the antitumor effects of DHT on ATC cells *in vitro*, alone and in combination with cisplatin. Despite these encouraging results, this study is limited by the lack of an *in vivo* model. Therefore, further and more detailed studies on its effects on HuR regulation, as well as *in vivo* investigation of this combination, are needed.

Acknowledgements

Not applicable.

Funding

No funding was received.

Availability of data and materials

The datasets used and/or analyzed during the current study are available from the corresponding author on reasonable request. Raw and processed data are available on the public online repository Gene Expression Omnibus (dataset no. GSE168616).

Authors' contributions

LA, FB, GD and DR conceived the study. LA designed the methodology. LA, MN, RD, FC, FB and MC performed the experiments and validated the data. FB, MN, FC and RD analyzed the data. LA and FB wrote the original draft. GD, MC, DR reviewed and edited the manuscript. GD and DR supervised the study. All authors read and approved the final manuscript. LA, FB and GD confirm the authenticity of all the raw data.

Ethics approval and consent to participate

Not applicable.

Patient consent for publication

Not applicable.

Competing interests

The authors declare that they have no competing interests.

References

1. Abe I and Lam AK: Anaplastic thyroid carcinoma: Updates on WHO classification, clinicopathological features and staging. Histol Histopathol 36: 239-248, 2021.
2. Lim H, Devesa SS, Sosa JA, Check D and Kitahara CM: Trends in thyroid cancer incidence and mortality in the United States, 1974-2013. JAMA 317: 1338-1348, 2017.
3. Amin MB, Edge SB, Greene FL, Byrd DR, Brookland RK, Washington MK, Gershenwald JE, Compton CC, Hess K, Sullivan DC, *et al*: Organization of the AJCC cancer staging manual. AJCC Cancer Staging Manual, pp31-37, 2017.
4. Nylén C, Mechera R, Maréchal-Ross I, Tsang V, Chou A, Gill AJ, Clifton-Bligh RJ, Robinson BG, Sywak MS, Sidhu SB and Glover AR: Molecular markers guiding thyroid cancer management. Cancers (Basel) 12: 2164, 2020.
5. Li Z, Zhang Y, Wang R, Zou K and Zou L: Genetic alterations in anaplastic thyroid carcinoma and targeted therapies. Exp Ther Med 18: 2369-2377, 2019.
6. Goutsouliak V and Hay JH: Anaplastic thyroid cancer in British Columbia 1985-1999: A population-based study. Clin Oncol (R Coll Radiol) 17: 75-78, 2005.
7. Pezzi TA, Mohamed ASR, Sheu T, Blanchard P, Sandulache VC, Lai SY, Cabanillas ME, Williams MD, Pezzi CM, Lu C, *et al*: Radiation therapy dose is associated with improved survival for unresected anaplastic thyroid carcinoma: Outcomes from the National cancer data base. Cancer 123: 1653-1661, 2017.
8. Prasongsook N, Kumar A, Chintakuntlawar AV, Foote RL, Kasperbauer J, Molina J, Garces Y, Ma D, Wittich MAN, Rubin J, *et al*: Survival in response to multimodal therapy in anaplastic thyroid cancer. J Clin Endocrinol Metab 102: 4506-4514, 2017.
9. Kim JH and Leeper RD: Treatment of locally advanced thyroid carcinoma with combination doxorubicin and radiation therapy. Cancer 60: 2372-2375, 1987.
10. Hosseini A and Ghorbani A: Cancer therapy with phytochemicals: Evidence from clinical studies. Avicenna J Phytomedicine 5: 84-97, 2015.
11. Shin HJ, Hwang KA and Choi KC: Antitumor effect of various phytochemicals on diverse types of thyroid cancers. Nutrients 11: 125, 2019.
12. Hosseinimehr SJ and Hosseini SA: Resveratrol sensitizes selectively thyroid cancer cell to 131-iodine toxicity. J Toxicol 2014: 839597, 2014.
13. Xu X, Qin J and Liu W: Curcumin inhibits the invasion of thyroid cancer cells via down-regulation of PI3K/Akt signaling pathway. Gene 546: 226-232, 2014.
14. Zhang L, Cheng X, Gao Y, Zhang C, Bao J, Guan H, Yu H, Lu R, Xu Q and Sun Y: Curcumin inhibits metastasis in human papillary thyroid carcinoma BCPAP cells via down-regulation of the TGF-β/Smad2/3 signaling pathway. Exp Cell Res 341: 157-165, 2016.
15. Chen X, Yu J, Zhong B, Lu J, Lu JJ, Li S and Lu Y: Pharmacological activities of dihydrotanshinone I, a natural product from *Salvia miltiorrhiza* Bunge. Pharmacol Res 145: 104254, 2019.
16. Wang L, Yeung JH, Hu T, Lee WY, Lu L, Zhang L, Shen J, Chan RL, Wu WK and Cho CH: Dihydrotanshinone induces p53-independent but ROS-dependent apoptosis in colon cancer cells. Life Sci 93: 344-351, 2013.
17. Tsai SL, Suk FM, Wang CI, Liu DZ, Hou WC, Lin PJ, Hung LF and Liang YC: Anti-tumor potential of 15,16-dihydrotanshinone I against breast adenocarcinoma through inducing G1 arrest and apoptosis. Biochem Pharmacol 74: 1575-1586, 2007.
18. Cheng R, Chen J, Wang Y, Ge Y, Huang Z and Zhang G: Dihydrotanshinone induces apoptosis of SGC7901 and MGC803 cells via activation of JNK and p38 signalling pathways. Pharm Biol 54: 3019-3025, 2016.
19. Chen X, Li Q, He Y, Du H, Zhan Z, Zhao H, Shi J, Ye Q and Hu J: 15,16-dihydrotanshinone I induces apoptosis and inhibits the proliferation, migration of human osteosarcoma cell line 143b in vitro. Anticancer Agents Med Chem 17: 1234-1242, 2017.
20. Liu JJ, Wu HH, Chen TH, Leung W and Liang YC: 15,16-Dihydrotanshinone I from the functional food *Salvia miltiorrhiza* exhibits anticancer activity in human HL-60 leukemia cells: In vitro and in vivo studies. Int J Mol Sci 16: 19387-19400, 2015.
21. Wang F, Ma J, Wang KS, Mi C, Lee JJ and Jin X: Blockade of TNF-α-induced NF-κB signaling pathway and anti-cancer therapeutic response of dihydrotanshinone I. Int Immunopharmacol 28: 764-772, 2015.
22. Lee DS and Lee SH: Biological activity of dihydrotanshinone I: Effect on apoptosis. J Biosci Bioeng 89: 292-293, 2000.
23. Ye Y, Xu W, Zhong W, Li Y and Wang C: Combination treatment with dihydrotanshinone I and irradiation enhances apoptotic effects in human cervical cancer by HPV E6 down-regulation and caspases activation. Mol Cell Biochem 363: 191-202, 2012.
24. Lal P, Cerofolini L, D'Agostino VG, Zucal C, Fuccio C, Bonomo I, Dassi E, Giuntini S, Di Maio D, Vishwakarma V, *et al*: Regulation of HuR structure and function by dihydrotanshinone-I. Nucleic Acids Res 45: 9514-9527, 2017.
25. Baldan F, Mio C, Allegri L, Conzatti K, Toffoletto B, Puppin C, Radovic S, Vascotto C, Russo D, Di Loreto C and Damante G: Identification of tumorigenesis-related mRNAs associated with RNA-binding protein HuR in thyroid cancer cells. Oncotarget 7: 63388-63407, 2016.
26. Allegri L, Mio C, Russo D, Filetti S and Baldan F: Effects of HuR downregulation on anaplastic thyroid cancer cells. Oncol Lett 15: 575-579, 2018.
27. Allegri L, Baldan F, Roy S, Aubé J, Russo D, Filetti S and Damante G: The HuR CMLD-2 inhibitor exhibits antitumor effects via MAD2 downregulation in thyroid cancer cells. Sci Rep 9: 7374, 2019.
28. Skoufias DA, Andreassen PR, Lacroix FB, Wilson L and Margolis RL: Mammalian mad2 and bub1/bubR1 recognize distinct spindle-attachment and kinetochore-tension checkpoints. Proc Natl Acad Sci USA 98: 4492-4497, 2001.
29. Heldin NE and Westermark B: The molecular biology of the human anaplastic thyroid carcinoma cell. Thyroidology 3: 127-131, 1991.
30. Ito T, Seyama T, Hayashi Y, Hayashi T, Dohi K, Mizuno T, Iwamoto K, Tsuyama N, Nakamura N and Akiyama M: Establishment of 2 human thyroid-carcinoma cell-lines (8305c, 8505c) bearing P53 gene-mutations. Int J Oncol 4: 583-586, 1994.
31. Landa I, Pozdeyev N, Korch C, Marlow LA, Smallridge RC, Copland JA, Henderson YC, Lai SY, Clayman GL, Onoda N, *et al*: Comprehensive genetic characterization of human thyroid cancer cell lines: A validated panel for preclinical studies. Clin Cancer Res 25: 3141-3151, 2019.

32. Mio C, Lavarone E, Conzatti K, Baldan F, Toffoletto B, Puppin C, Filetti S, Durante C, Russo D, Orlacchio A, *et al*: MCM5 as a target of BET inhibitors in thyroid cancer cells. Endocr Relat Cancer 23: 335-347, 2016.
33. Justus CR, Leffler N, Ruiz-Echevarria M and Yang LV: In vitro cell migration and invasion assays. J Vis Exp: 51046, 2014.
34. Martin M: Cutadapt removes adapter sequences from high-throughput sequencing reads. EMBnet J 17: 10-12, 2011.
35. Del Fabbro C, Scalabrin S, Morgante M and Giorgi FM: An extensive evaluation of read trimming effects on Illumina NGS data analysis. PLoS One 8: e85024, 2013.
36. Dobin A, Davis CA, Schlesinger F, Drenkow J, Zaleski C, Jha S, Batut P, Chaisson M and Gingeras TR: STAR: Ultrafast universal RNA-seq aligner. Bioinformatics 29: 15-21, 2013.
37. Pertea M, Pertea GM, Antonescu CM, Chang TC, Mendell JT and Salzberg SL: StringTie enables improved reconstruction of a transcriptome from RNA-seq reads. Nat Biotechnol 33: 290-295, 2015.
38. Lombardo GE, Maggisano V, Celano M, Cosco D, Mignogna C, Baldan F, Lepore SM, Allegri L, Moretti S, Durante C, *et al*: Anti-hTERTsiRNA-Loaded nanoparticles block the growth of anaplastic thyroid cancer xenograft. Mol Cancer Ther 17: 1187-1195, 2018.
39. Livak KJ and Schmittgen TD: Analysis of relative gene expression data using real-time quantitative PCR and the 2(-Delta Delta C(T)) method. Methods 25: 402-408, 2001
40. Darzynkiewicz Z, Bruno S, Bino GD, Gorczyca W, Hotz MA, Lassota P and Traganos F: Features of apoptotic cells measured by flow cytometry. Cytometry 13: 795-808, 1992.
41. Mi H, Ebert D, Muruganujan A, Mills C, Albou LP, Mushayamaha T and Thomas PD: PANTHER version 16: A revised family classification, tree-based classification tool, enhancer regions and extensive API. Nucleic Acids Res 49: D394-D403, 2021.
42. Shakib H, Rajabi S, Dehghan MH, Mashayekhi FJ, Safari-Alighiarloo N and Hedayati M: Epithelial-to-mesenchymal transition in thyroid cancer: A comprehensive review. Endocrine 66: 435-455, 2019.
43. Genga KR, Filho FD, Ferreira FV, de Sousa JC, Studart FS, Magalhães SM, Heredia FF and Pinheiro RF: Proteins of the mitotic checkpoint and spindle are related to chromosomal instability and unfavourable prognosis in patients with myelodysplastic syndrome. J Clin Pathol 68: 381-387, 2015.
44. Yu L, Guo WC, Zhao SH, Tang J and Chen JL: Mitotic arrest defective protein 2 expression abnormality and its clinicopathologic significance in human osteosarcoma. APMIS 118: 222-229, 2010.
45. Wada N, Yoshida A, Miyagi Y, Yamamoto T, Nakayama H, Suganuma N, Matsuzu K, Masudo K, Hirakawa S, Rino Y, *et al*: Overexpression of the mitotic spindle assembly checkpoint genes hBUB1, hBUBR1 and hMAD2 in thyroid carcinomas with aggressive nature. Anticancer Res 28: 139-144, 2008.
46. Tanabe S, Aoyagi K, Yokozaki H and Sasaki H: Gene expression signatures for identifying diffuse-type gastric cancer associated with epithelial-mesenchymal transition. Int J Oncol 44: 1955-1970, 2014.
47. Wu H, Sun Y, Ye H, Yang S, Lee SL and de las Morenas A: Anaplastic thyroid cancer: Outcome and the mutation/expression profiles of potential targets. Pathol Oncol Res 21: 695-701, 2015.
48. Fan D, Ma J, Bell AC, Groen AH, Olsen KS, Lok BH, Leeman JE, Anderson E, Riaz N, McBride S, *et al*: Outcomes of multimodal therapy in a large series of patients with anaplastic thyroid cancer. Cancer 126: 444-452, 2020.
49. Bulotta S, Celano M, Costante G and Russo D: Emerging strategies for managing differentiated thyroid cancers refractory to radioiodine. Endocrine 52: 214-221, 2016.
50. Ljubas J, Ovesen T and Rusan M: A Systematic review of phase II targeted therapy clinical trials in anaplastic thyroid cancer. Cancers (Basel) 11: 943, 2019.
51. Rigalli JP, Tocchetti GN, Arana MR, Villanueva SS, Catania VA, Theile D, Ruiz ML and Weiss J: The phytoestrogen genistein enhances multidrug resistance in breast cancer cell lines by translational regulation of ABC transporters. Cancer Lett 376: 165-172, 2016.
52. Bespalov VG, Alexandrov VA, Semenov AL, Vysochina GI, Kostikova VA and Baranenko DA: The inhibitory effect of *Filipendula ulmaria* (L.) Maxim. on colorectal carcinogenesis induced in rats by methylnitrosourea. J Ethnopharmacol 227: 1-7, 2018.
53. Samec M, Liskova A, Kubatka P, Uramova S, Zubor P, Samuel SM, Zulli A, Pec M, Bielik T, Biringer K, *et al*: The role of dietary phytochemicals in the carcinogenesis via the modulation of miRNA expression. J Cancer Res Clin Oncol 145: 1665-1679, 2019.
54. Kapinova A, Kubatka P, Golubnitschaja O, Kello M, Zubor P, Solar P and Pec M: Dietary phytochemicals in breast cancer research: Anticancer effects and potential utility for effective chemoprevention. Environ Health Prev Med 23: 36, 2018.
55. Schwertheim S, Wein F, Lennartz K, Worm K, Schmid KW and Sheu-Grabellus SY: Curcumin induces G2/M arrest, apoptosis, NF-kappaB inhibition, and expression of differentiation genes in thyroid carcinoma cells. J Cancer Res Clin Oncol 143: 1143-1154, 2017.
56. Allegri L, Rosignolo F, Mio C, Filetti S, Baldan F and Damante G: Effects of nutraceuticals on anaplastic thyroid cancer cells. J Cancer Res Clin Oncol 144: 285-294, 2018.
57. Hu T, Wang L, Zhang L, Lu L, Shen J, Chan RL, Li M, Wu WK, To KK and Cho CH: Sensitivity of apoptosis-resistant colon cancer cells to tanshinones is mediated by autophagic cell death and p53-independent cytotoxicity. Phytomedicine 22: 536-544, 2015.
58. Tan S, Hou X and Mei L: Dihydrotanshinone I inhibits human glioma cell proliferation via the activation of ferroptosis. Oncol Lett 20: 122, 2020.
59. Wang X, Xu X, Jiang G, Zhang C, Liu L, Kang J, Wang J, Owusu L, Zhou L, Zhang L and Li W: Dihydrotanshinone I inhibits ovarian cancer cell proliferation and migration by transcriptional repression of PIK3CA gene. J Cell Mol Med 24: 11177-11187, 2020.
60. Bates M, Spillane CD, Gallagher MF, McCann A, Martin C, Blackshields G, Keegan H, Gubbins L, Brooks R, Brooks D, *et al*: The role of the MAD2-TLR4-MyD88 axis in paclitaxel resistance in ovarian cancer. PLoS One 15: e0243715, 2020.
61. Pajuelo-Lozano N, Alcalá S, Sainz B Jr, Perona R and Sanchez-Perez I: Targeting MAD2 modulates stemness and tumorigenesis in human Gastric cancer cell lines. Theranostics 10: 9601-9618, 2020.
62. Nascimento AV, Singh A, Bousbaa H, Ferreira D, Sarmento B and Amiji MM: Overcoming cisplatin resistance in non-small cell lung cancer with Mad2 silencing siRNA delivered systemically using EGFR-targeted chitosan nanoparticles. Acta Biomater 47: 71-80, 2017.
63. Seto A, Sugitani I, Toda K, Kawabata K, Takahashi S and Saotome T: Chemotherapy for anaplastic thyroid cancer using docetaxel and cisplatin: Report of eight cases. Surg Today 45: 221-226, 2013.
64. Ranganath R, Shah MA and Shah AR: Anaplastic thyroid cancer. Curr Opin Endocrinol Diabetes Obes 22: 387-391, 2015.
65. Celano M, Maggisano V, Bulotta S, Allegri L, Pecce V, Abballe L, Damante G and Russo D: Quercetin improves the effects of sorafenib on growth and migration of thyroid cancer cells. Endocrine 67: 496-498, 2020.